

Breast Cancer Cell Identification and Measurement from NSOPL of Nir Back Scattering Signals

¹S. Yuvarani and ²C. Jothi Venkateswaran

ABSTRACT

In this paper, cancer cell of size below 5mm are detected and measured from breast phantom. Detection of cell is from back sprinkled signals of 850 nm Near Infra Red (NIR) radiation wavelength from phantom. Measurements of cells in different sizes obtained from Nano Size Optical Path Length (NSOPL) of difference in signals, collected from with and without cancer cell phantom. However, cancer cells of size below 5mm detection are a challenging task for the radiologist. For the size of cells below 5mm, the radiation from various diagnosing instruments either break the cancer cells or not able to capture in the DICOM images. From 450 number of back scattered signals of near field Infra Red optical radiation taken for Diagnosis and measurement of micro cancer cells. From the results, we can measure the cell with 90% in accuracy.

Keywords: NIR diodes, OPL, Backscattering, breast cancer cell, breast phantom

INTRODUCTION

Cancer in human body, which develops from tissues in particular area, causes illness. Breast Cancer makes a change in shape, lump, fluid coming from the nipple, dimpling of the skin or a red scaly patch of skin. Breast cancer occurs due to lack of physical exercise, female sex, drinking alcohol, ionizing radiation, and hormone replacement therapy during menopause, early age menstruation, not at all or having children late and older age. Generally, parent genes inherit 5 – 10 % of cases. Breast cancer commonly develops from cells, which engage in supplying the ducts of milk, lobules and lining of milk ducts. The tissues from ductal carcinomas from ducts lead to cancer, developing from lobules known as lobular carcinomas. Mostly cancer develops from ductal carcinoma in situ and pre-invasive lesion. Initially cancer is identified from the biopsy to diagnosis the concerning lump.

All types of breast cancer diagnosed with biopsy and microscopic analysis. Rare types of breast cancers that require some experiments and lab exams. To detect the breast cancer common methods are commonly screening, physical examination of breast through the health provider and mammography. Generally, microscope detects breast cancer cells. Outcomes for breast cancer vary depending on the cancer type, extent of disease, and person's age. The types of cancer are Invasive ductal carcinoma, Invasive lobular carcinoma, Phyllodes tumor, Angiosarcoma & Ductal carcinoma in situ. Invasive ductal carcinoma cancer infiltrates and starts in a milk duct of the breast, breaks from side to side the wall of the duct, and grows into the fatty tissue of the breast. At this point, it may be able to increase (metastasize) to other parts of the body through the lymphatic system and bloodstream. Invasive lobular carcinoma (ILC) starts in the milk-producing lobules. Like IDC, it can spread to other parts of the body. About 1 in 10 invasive breast cancers is an ILC. Invasive lobular carcinoma may be harder to detect through mammogram than invasive ductal carcinoma. Phyllodes tumour in breast tumour develops in the connective tissue of the breast, in contrast to carcinomas,

¹ Research Scholar, Research and Development Centre, Bharathiar University, Coimbatore, Tamilnadu, India.

² Assistant Professor & Head, Department of Computer Science, Presidency College, Chennai-600 005, Tamil Nadu, India.

which develop in the ducts or lobules. Other names for these tumours include phylloides tumour and cystosarcoma phyllodes.

These tumours are usually benign but on rare occasions may be malignant. A malignant phyllodes tumour treated with removal of wider margin of normal tissue. Surgery is necessary, but these cancers might not respond as well to the other treatments used for more common breast Angiosarcoma cancer starts in cells that line blood vessels or lymph vessels. When it does, it usually develops as a complication of previous radiation treatments. Rare complication of breast radiation therapy that can develop about 5 to 10 years after radiation. Angiosarcoma can also occur in the arms of women who develop lymphedema because of lymph node surgery or radiation therapy to treat breast cancer. Ductal carcinoma considered has non-invasive or pre-invasive breast cancer. DCIS means that cells that lined the ducts have changed to look like cancer cells. The difference between DCIS and invasive cancer is that the cells have not spread through the walls of the ducts into the surrounding breast tissue. DCIS is a pre-cancer because some cases can go on to become invasive cancers.

RELATED WORKS

Mammographic images are present in low quality contrast, so to detect symptoms of cancer and find micro-masses and classification is difficult. A novel algorithm to identify micro-masses and classification has the steps as follows 1) Extraction of texture feature in entropy, mean, kurtosis etc, 2) Mass region extraction to get exact shape of mass 3) Superposition of boundary of mass helps to cover boundary easily in overlaps region of parenchyma. Algorithm processed on fourteen patients, six patient's cancer extracted and detect clear mass image [1]. Early detection of breast cancer through the mammograms, leads to early treatment and improves perpetuation rates to great magnitude. Inter and intra-observer errors take place continuously in medial image study and high variability between elucidations of different radiologists. The radiologist's refinement of mammographic varies with image quality and proficiency of the procedures, efforts taken to automate the typecasting and diagnosis of breast cancer images. To overview infection areas in breast cancer images, computer-aided diagnosis (CAD) mammograms, and focus on the mathematical aspects [2]. Computer Aided Design (CAD) based systems aid radiologists in comfort way to classify the malignant or benign as mammography (tumour). To detection of breast cancer need features extraction from mammography with CAD systems. New feature-set is involving mammographs and six pre-existing. Minima as database used to store and retrieve images to apply a cases included 5-speculated and 4-circumscribed malignant lesions, 9-speculated and 16-circumscribed benign lesions. The Kohnan neural network detects the features of cases. From result, 80% classification rate attained [3]. Image processing technique, watershed transform widely applied in ultrasound and x-ray to provide enhance medical images, mainly focus on breast cancer. The proposed algorithm based on segmentation watershed transformation morphological operation, to diagnosis of breast tumour in all types of medical images. The algorithm tested in X-ray, ultrasound images and obtained enhances results for breast cancer [4]. Small clusters of micro classification appearing as white spots shows in mammograms gives an early warning of breast cancer and also shows importance of mammography in breast cancer to detected in early stage of cancer to prevent critical situation. Early detection of disease from X-ray based mammography provides key to improve prognosis and develops the radiologists diagnostic.

A radiologist diagnostic and other techniques performance's are improved through a computer-aided diagnosis (CAD) schemes help to detect primary signatures. An improved CAD tools developed to describe a masses and micro calcification, shapes belongs to masses space-occupying lesions, denseness, and margins properties. To detect breast cancer through mammography with their benign glandular tissue and masses, to show interest on low contrast images in micro and masses classifications with tiny deposits of calcium that appears in small the bright spots. To mass segmentation on cancer tumour, fuzzy c – means clustering (FCM) implemented on cancer signs and its intensity on background tissue (morphological operators) [5].

Multiple Circular Path Convolution Neural Network architecture analyze for tumour. Initially tumour area divided into a sector, each sector is computed mass features independently. These independent sectors acts as input layer, coordinated with different sizes through convolution kernels that propagated signals to the neural network system second layer. A dual morphological enhancement technique selects mammograms randomly for processing, region growing algorithm isolated radio dense areas. Calculate region of interest, each boundary divided into 36-equai-angular dividers, and sectors radiated from centre of the region with invented neural network system computed with 144 – Breast Imaging-Reporting and Data System features as input values for evaluation. A performance of A z values markedly enhance from 0.78-0.80 to 0.84-0.89 under MCPCNN compared from conventional feed-forward neural network. Therefore, MCPCNN set better performance in analysis of mass features [6]. Algorithm combines artificial intelligent techniques and discrete wavelet transform (DWT) for visually detection masses in mammograms.

The procedure includes AI techniques, which belongs to dogs-and-rabbits algorithm, fractal dimension analysis, multi-resolution Markov random field and others. The futures mainly used to find a cancerous tumour type, which embedded in varying densities of parenchymal tissue structures, difficult in mammograms. In AI techniques, dogs-and-rabbits clustering algorithm initiate segmentation at LL sub-band of DWT (three level) decomposition of the mammogram. A fractal dimension analysis determined regions of cancer approximately in the mammogram. The proposed algorithm verified with 322 mammogram images in Mammographic Image analysis Society Database, show results in sensitivity of 97.3% and 3.92 in number of false positives per image [7]. An objective to find out an algorithm, that algorithm results are more suitable for specific application compared to an original image. Digital image enhancement techniques concepts provide a multitude of choices for improving visual quality of images. To enhance mammogram images, frequency domain smoothing-sharpening techniques aim to gain sharpening process and monitor changes in the image intensity. This technique applied to remove random noise from digital images. For specific application eliminates the drawbacks of each smoothing and sharpening techniques in image processing field. To enhance X-ray mammograms for breast cancer and advantageously aid to radiologists to detect an improved image contrast [8]. Neural Network experimental system concerns planer and cylindrical configurations of a microwave imaging system. A microwave imaging system includes step-frequency synthesized pulse for detection of breast cancer.

A system with simple phantom, consisting of cylindrical plastic container emulating tumour through highly reflective object and low dielectric constant imitating fatty tissues. Different calibration scale on system for successful detection of the target [9]. In recent years especially wideband (UWB) microwave imaging system is alterative and an important to mammography and other techniques such as ultra sound in breast cancer detection or magnetic resonance imaging. A UWB microwave imaging based on two fundamental properties, initially tumours are highly water content compare with normal breast tissues, and it is as higher dielectric constant. A microwave imaging system helps to detect early-stage tumour, when initial or too small size, because attenuation of microwave is too low 4.5 dB/cm in range of 3.1 to 10.6 GHz UW frequency band. Therefore, UWB microwave imaging permits detection tumours in high dynamic range of the breast radar, this system approaches imaging to employ an illuminating device (an antenna), and medium between an imaged object. Due to this medium, minimizes the declaration and lively range of the imaging system. Mainly researchers concrete on dielectric constant and optimal characteristics of coupling medium of skin or normal tissue [10]. To identifying normal tissue in mammograms, an algorithm to digitized normal regions and abnormal regions. This algorithm serves as recognition of density of normal tissue regions and statistical distribution directly depends upon one parameter with distribution function. In this summary statistics used to set detection error rates.

A spatial filters process matched to resolution with each expansion image independently. Above concept and algorithms are ultimately leads to automated algorithm for identification of digital or normal mammograms [11]. Wavelet method of image enhancement to modifying the coefficients to remove noise

from data. The concepts use processing digitalized x-ray image that enhance the amount of detail visible in x-ray image processing in computerized system.

The effect of this method used to diagnose early malignant tumours for effective action and detection of invisible mass. The mammograms detect small percentage of the information due to minor difference in x-band attenuation between normal malignant diseases and glandular tissues. To detect small malignancies is too difficult and processing digital medical image processing uses image enhancement and de-noising may not be obvious and help the oncologist to decide [12]. Image texture analysis, texture image segmentation and image compression processes with fractal analyses. A two class's malign at and benign are classify the breast lesions in system based fractal analysis by computer-aided diagnosis. A fractal Brownian motion estimates fractal dimension of an ultrasound images, that images are consists difference in neighboring pixels of gray value. To increase the efficiency of fractal analysis, histogram equalization and morphology operations applied in image. Finally, classify benign tumours from malignant using K-means classification method [13]. In worldwide, cancer is leading cause to human being, so early detection of causes is important to secure people from cancer and provide diagnosis and treatment techniques. Computerized ultrasound screening techniques to detect beginning and malignant tissue and to diagnose the cancer, because ultrasound techniques screen detail image function and structure of the image in the real time entity [14]. Microwave-based methods and neural networks with wavelet analyses an image to show improve results in breast detection. Here one of the improved techniques like hybrid model in combination of acoustic signals and microwaves to improve the detection capability [15]. Moreover, Survival rates of Breast cancer patients, high, between 80% and 90% in England. In developing countries, survival rates are low. Worldwide, breast cancer is the most important type of cancer in women, accounting for 25% of all cases. A healthy diet & exercise routine can reduce the chance for breast cancer nearly 40%, earlier detection of breast cancer has 98% of survival rate. Nearly 85% of women diagnosed with breast cancer in USA, does not have family history. Over 2 Million women in USA diagnosed with breast cancer in previous stage, treated. The earlier stage, treatment for cancer remains a challenging task, and this problem approached with a novel method based on NIR Backscattered signal from cancer cells.

METHODOLOGY

The detection of breast cancer with the instruments such as optical, microwave, ultrasound, manual testing are not able to detect the cancer cells size below 5mm of diameter. The detection of the minimum size cancer cells with UWB radar imaging and serum tests developed by the researchers until today. Still none of the methods is standard method. The earlier detection of cancer cells i.e., the cell in smaller would be a challenging task for the researchers. To solve this problem, in this paper a novel approach with the NIR sensors and DyDWT deployed to detect the smaller diameter cells in the breast. The Figure 1 shows the block diagram of the methodology. The optical properties can diagnosis and therapeutic the diseases. In diagnosis, the light can pass through the tissue and interrogate the components in tissue, then comes out of tissue, the light comes out of the tissues are collected in the form of signal or image for diagnosis. The aptitude of light to deposit power in the tissue based on absorption properties is the key for therapeutic application. The scattering property of optical light from breast tissues measured with detector diodes in NIR wavelength for cancer cell detection. The scattering behaviour of light measured with optical path length. The scattering of optical light from the particles occurs when the refractive index is different from the surrounding medium. The characterize of the cancer cell behaviour of scattering co-efficient of tissues would be given by the equation below

$$U'(s) = a (\lambda/500(\mu\text{m}))^{-b} \quad (1)$$

Scattering co-efficient of tissues is $U'(s)$ and 'b' the scattering power and 'a' scales the wavelength-dependent term.

Breast Phantom

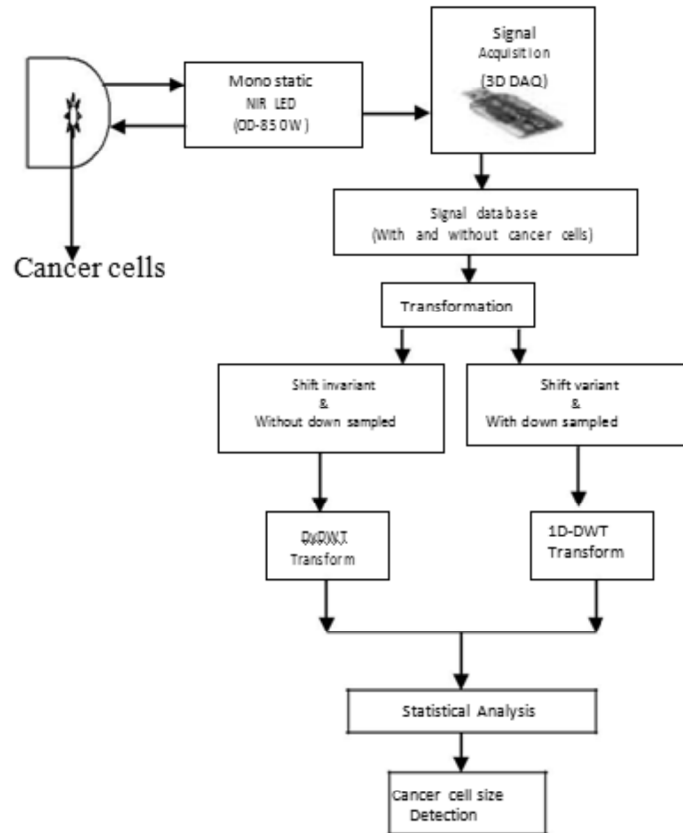


Figure 1: Methodology block diagram of cancer cell detection.

For experimental study, the breast tissues are in the form of petroleum jelly of 150gms. The petroleum jelly collected in glass container, the permittivity and conductivity properties of the jelly are 2.36, and 0.012. The glass container is of 2mm thickness and 10mm of diameter and forms the skin region of breast. The glass container and the petroleum jelly form the breast phantom. The breast phantom contains without and with cancer cell utilized for this study. The cancer cell contains a mixture of wheat and water. For the study, cell of 1mm to 5mm diameter samples taken. The cancer cell kept inside the tissue layer of the phantom in different locations. The cells in different locations focused with collated NIR Transmitter and Receiver for signal acquisition through 3D DAQ board. The 3D DAQ consist of Digital Class B power amplifier and capable for acquiring 3D signals.

The size of the device is of (0.5x0.9x2in). The digital Class B Power amplifier produces a good power gain. The power gain could able to describe the change of output power of the signal over a whole frequency of signal. The various frequencies and their powers compared with a specific frequency so the lower frequency component of the signal frequency variation is distinguished. The NIR LED of part No OD-850W sensor for detecting the cancer cell. The sensor features are high optical output with 850nm of peak emission. The sensor radiation angles cover a large are due to wide-angle emission. The single LED sensor run with fault could allow the maximum power output, with 7mm aperture 14mm from the emitting surface, the power passing through the aperture as the current is increased to maximum. The power output of NIR LED are eye safety LED. The methodology block diagram shows the picture of 3D DAQ in signal acquisition section. The DAQ acquired signals given as an input signal for DyDWT and 1D wavelet transform. The important property of DyDWT is not time sampled, when compared with the other transforms. The DyDWTs are scaled samples of any wavelet transform, with a geometric sequence of ratio 2. This transform's shift

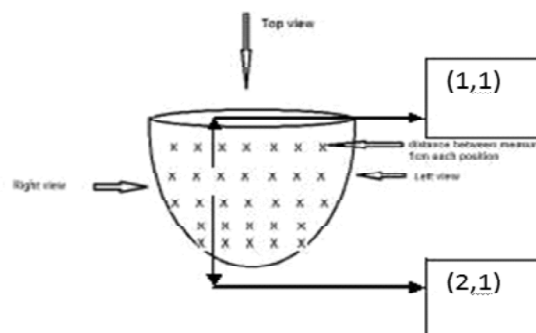
invariant property plays a vital role in reconstruction of the signal and no down sampling in sub band coding. Using these properties of DyDWT, the low frequency of the reflecting signals from cancer cells estimates clearly. The estimation of low frequency signals are difficult in other transforms are due to several scaling of co-efficient. The 1D DWT decomposes the input signal into two sub bands and the sub bands are low and High frequency components. The low and high frequency parts filtered with low pass and high pass filter and then down sampled with two. These down sampled signals are up sampled and filtered with low pass and high pass filter to synthesis. These synthesis filter signals are add to obtain the 1 D wavelet transformed output signals. Since the signals are 1D transform, the perfect reconstruction of filter obtained. The perfect reconstruction filter gives more details of the low frequency signals. The perfect reconstruction filter property are in both 1D and DyDWT transform and provides the better results for detecting the various diameters of cancer cells. The signals obtained from the phantom with and without various diameter cell evaluated statistically in LSSVM for separation and detection of the sizes of cancer cells.

EXPERIMENTS

The Figure 2 (a) shows the experimental setup photograph. The breast cancer cells below 5mm diameter detected with mono static NIR sensor acquired signals. The Mono static NIR sensor position in the phantom are shown in the Figure 2 (b). The location of NIR sensor in the Breast phantom are marked in the Figure 3 as 'X'. The marked position in the phantom forms matrix like structure for placing the Mono static NIR sensors. The matrix structure with 5x7 spots are the sensor positioned to collect the signal from the phantom with and without cancer cells. One centimeter distance between the spots in the phantom maintained for acquiring the signals. The acquisition of signals from top view, right view and bottom view from the Phantom with and without cancer cells forms a database of signals. The database consists of 450 signals totally, in which 448 signals are cancer cells and 2 signals are without cancer cells.



(a)



(b)

Figure 2: (a) The photograph of the experimental setup (b) Spots of Sensor Location for 5X7

The collected signals from the database taken as input for the DyDWT transform. Dyadic analysis filters bank collection of more band-limited components of dividing the frequency range. Typically, asymmetric and symmetric filter

banks structures. Filters are commonly sampling input frequency with half-band filters and $F/4$ cut-off frequency. Therefore, filters stop other filter passes frequency. It constructs for wide-band signals, unit takes adjacent high frequency and sub bands of lower frequency range and twice the output sample rate. The signals from the database transform with 1D DWT. The 1D transform has the property of shift variant with down sampled which can distinguish the optical path length to measure the cell size.

OPTICAL PROPERTIES OF CANCER CELLS

The Figure 3(a) shows the Back scattered signal of the acquired from the cancer cell phantom. The figure 3(b) shows the reconstructed Back scattered signal from DyDWT. The output signal of the transform shows with more number of bins in the figure. The more Bins in the plot are due to the reflected signal from the cancer cells. The cancer cell scatters the 850nm of wavelength radiation as non-coherent signal with low frequency.

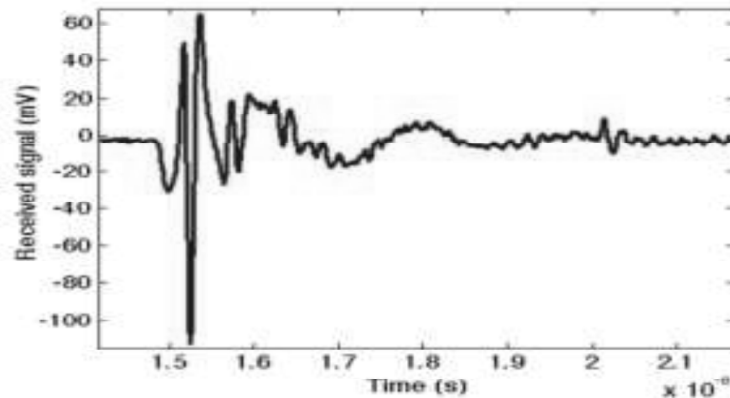


Figure 3 (a)

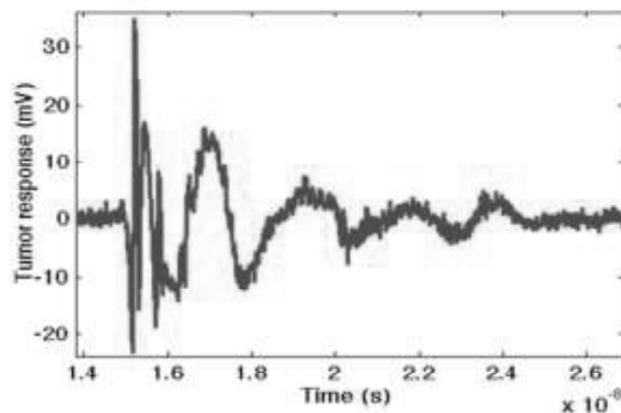


Figure 3 (b)

Figure 3(a) Back Scattered signal of cancer cell from phantom (b) DyDWT Back Scattered signal of cancer cell from phantom

The low frequency signal with different frequencies represents the presence of the cancer cells. The Statistical values of the low and high frequency signals correlated to the size of cancer cells. The Figure 4(a) shows back scattered signal of phantom without cancer cells. The Figure 4(b) shows the input signal processed with 1D DWT and DyDWT transform, reflected from 1m cancer cell phantom in the Right view

position at (1,1) spot. The Figure 4(c) shows the overlapping of 1mm cancer cell and DyDWT processed signal. From the overlapping signal of the input and processed signal, shows a difference in the frequency spectrum. The designated interval of the time record signals are consecutive analyzed with blocks of the time data for spectrum calculated from the signal. The 1mm cancer cell signal processed with lifting based 1D DWT for perfect reconstruction. The lifting 1D DWT can achieve a perfect reconstruction signals due to filters applied to divided signals. Then the divided signals operated with a series of convolution-accumulation to obtain the perfect reconstruction.

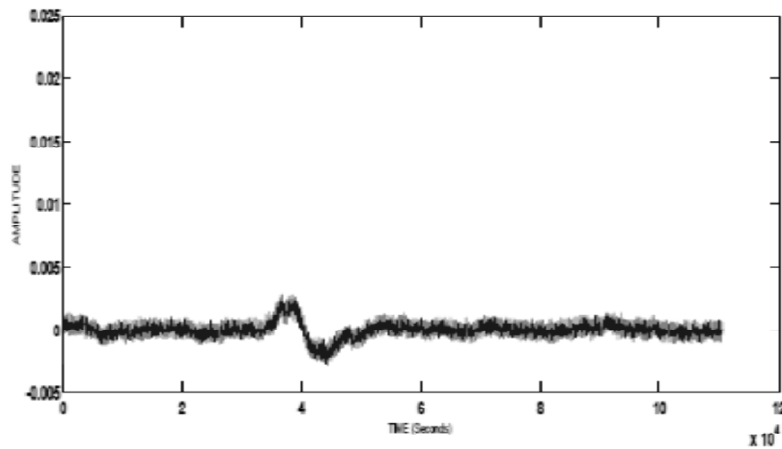


Figure 4(a): Signal from phantom without cell

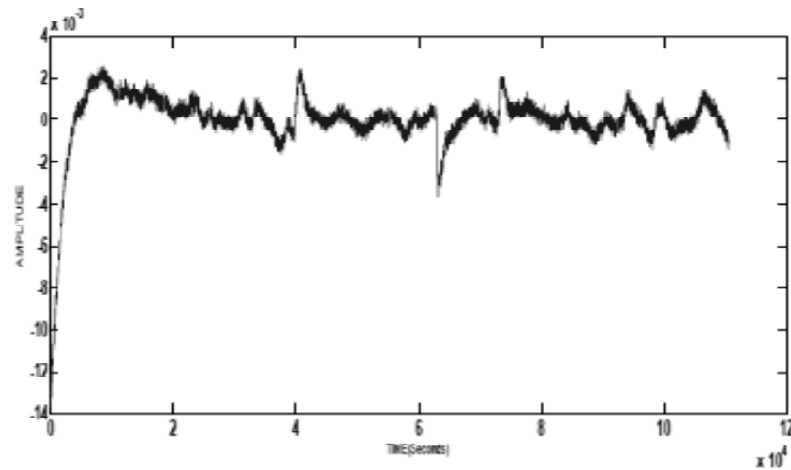


Figure 4(b): signal from 1mm cancer cell

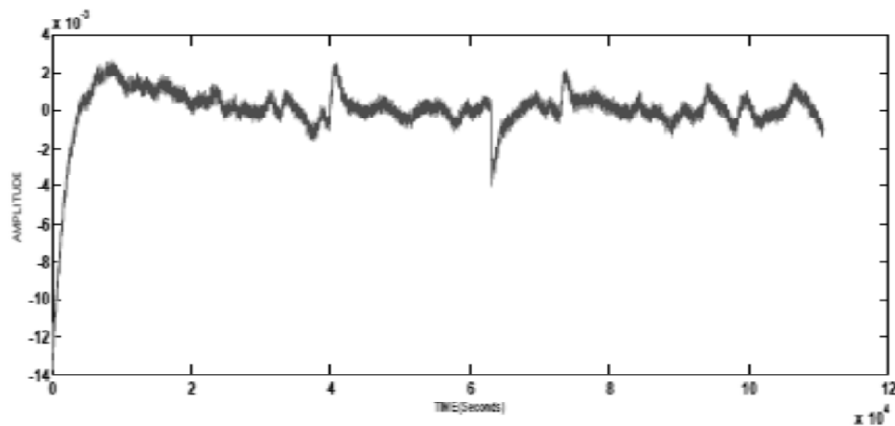


Figure 4(c): Overlay of 1mm cancer cell signal and DyDWT processed signal

The basic lifting scheme has implemented as follows

- (i) The pair of filters (a,b) us complementary then the perfect reconstruction can be executed.
- (ii) The for every filter q the pair (a',b) with $a'(z)=a(z)+q(Z^2).b(z)$ allows for perfect reconstruction.

Similiarly $b'(z)=b(z)+t(Z^2).a(z)$. The converse is also true, if (a,b) and (a',b) allow perfect reconstruction, the unique filter q with $a'(z)=a(z)+q(Z^2).b(z)$, each filter bank is called lifting step.

The lifting steps consists of varying lifts (ie.) once low pass filter is fixed and high pass is varied and in the next high pass will be fixed and low pass will be varied. The following procedure applied to the same direction and merged. The property of performing immediately in the memory of the input data with constant memory can able to bring different spectrum of the signal.

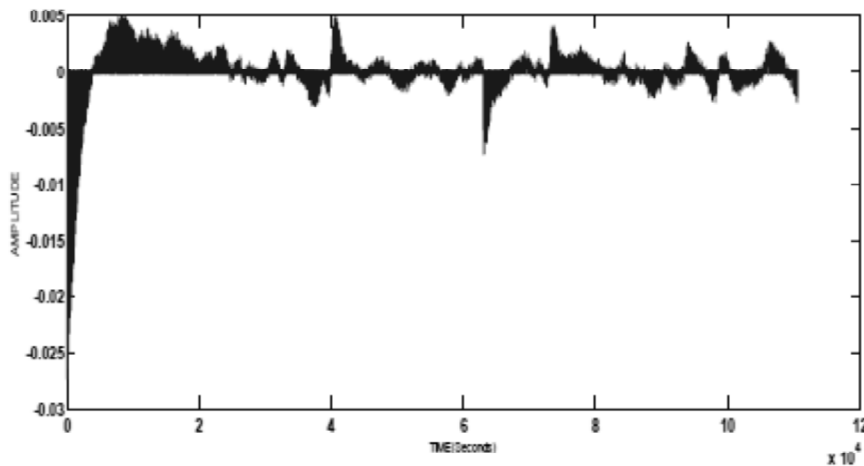


Figure 4(d): 1D processed signal

NIR diodes called as reflected infrared. Totally 500 signals collected from different size of cancer cells ranging from 1mm to 5mm to study the reflection properties . From the signal analysis of without cancer cells and with cancer cells, we found that the NIR wavelength ranging from 650nm to 950nm are absorbed by the water, lipids, chromophores and indocyanine. Besides the light absorbstion, there is a strong scattering of IR rays over the surface of tissue. Tissues are radiation scattering medium, this is shown in the Figure 5(a) of 2mm of cancer cell scattering. The Figure 5(b) and 5(c) shows the overlay of the signal and ID processed signal. The 450 processing-signals with cancer cells and without cancer cells show that “optical path length” changes with tissue size, types, and measuring geometry. The tissue size and measuring geometry obtained from quantitative spectral information. From results of 500-processed signal, optical path length changes to the size of cancer cell. The optical path length changes in nano scales with respect to size of the

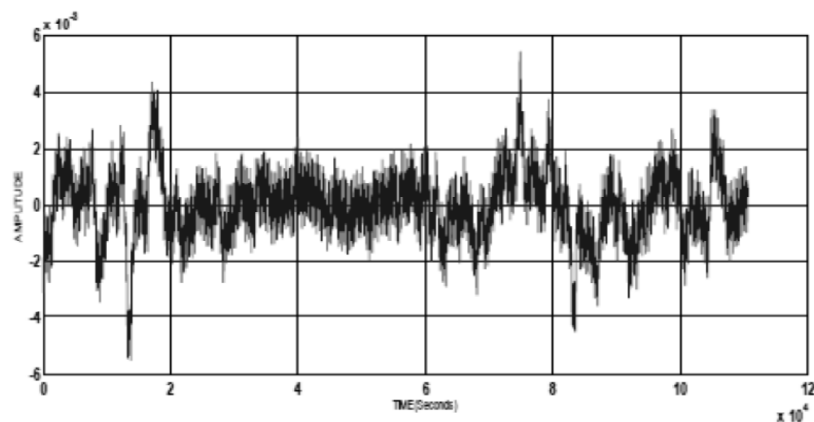


Figure 5(a): Signal from 2mm cancer cell

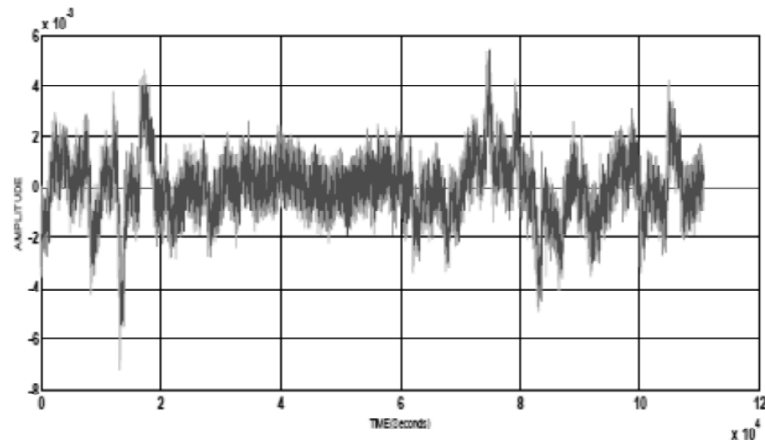


Figure 5 (b): Overlay of 2mm cancer cell signal and DyDWT processed signal

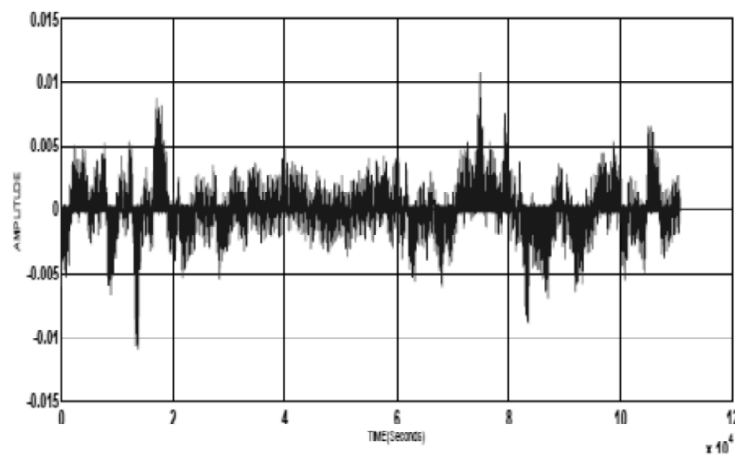


Figure 5(c): 1D processed signal

1mm and 2mm size of cancer cells, where as OPL are in micro scale for cancer cell above 3nm size. These nano scale ODL are filter with Dyadic wavelet and 1D DWT transform.

NANO SCALE OPTICAL PATH LENGTH MEASUREMENT

The nano scale OPL would be measurement with probability density function and standard normal distribution. The measurement of nano scale OPL for cancer cell size detections. The scattered signals are complex and the phase of signals affected with inherent random noise. The phase noise removal from the signals implemented with pdf. The intensity and phase of signals estimated with standard normal distribution. The inherent random noises in the scattered signal add when the scattered signals pass through the homogenous jelly region and enter the NIR detector. The random noise is less when the cell located near the glass region. The Nano scale OPL analysis with spectrum of signal. The spectrum of the signal for 1mm, 2mm and 5mm cells are shown in figure 6(a),6(b) and 6(c). A spectrogram figure shows how the frequency of the scattering signals change with the time. The amount of energy in signals with time and frequency in the figure shows in terms of dB. The frequency regions with small energy are in red colour, and the scattering of signals causes the energy of dark yellow region.

The Figure 6(a) of signal spectrum shows the narrow band spectrum for 1mm cells and has less scattering co-efficient. The Figures 6(b) and 6(c) shows the wideband spectrogram in the plot, which clearly shows the high scattering effect for the 2mm and 5mm cells. The typical variations seen in 3mm and 4mm cells signals in the database. The narrow band spectrogram is useful for detection of 2 and 3 mm and above the

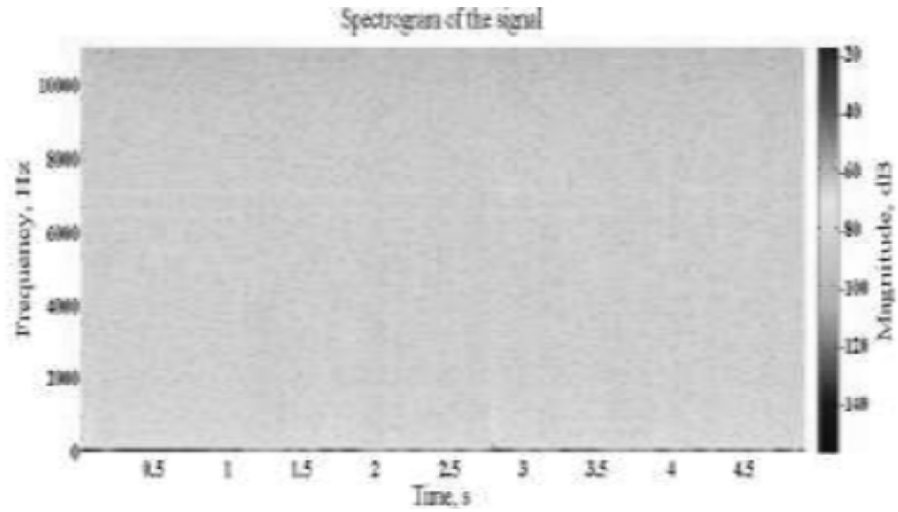


Figure 6(a): 1mm cancer cell signal spectrogram

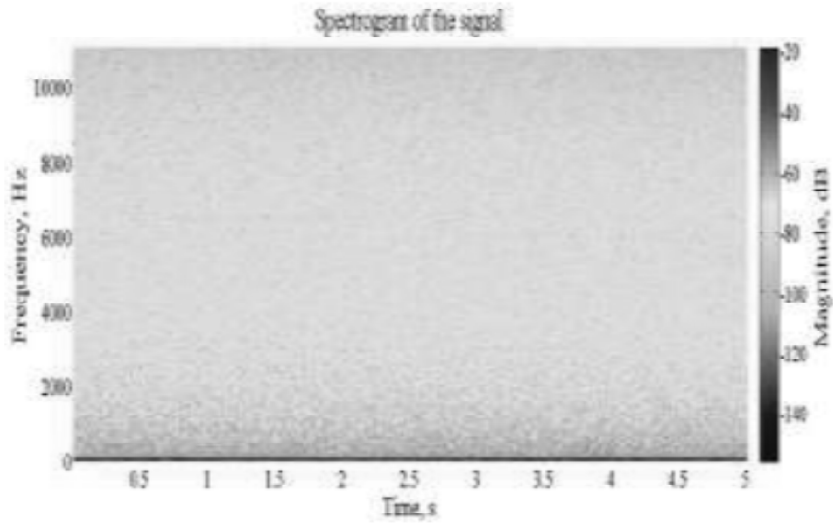


Figure (b): 2mm cancer cell signal spectrogram

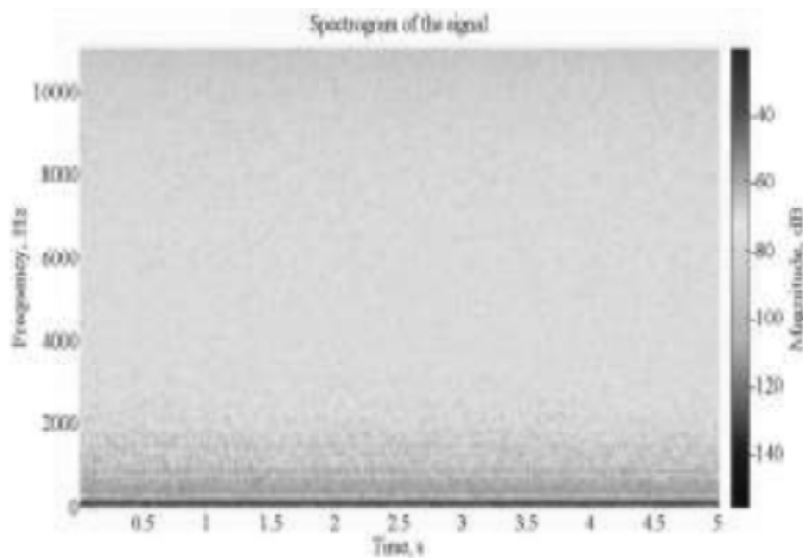


Figure (c): 5mm cancer cell signal spectrogram

spectrum shows wideband characteristics. From the colour of the spectrogram, we would be able to predict at which time and location the cancer cells are located in 'X' marked points in the phantom. The transformed signals are complex valued which represents the magnitude (ρ) and phase (θ) at a particular location and time. The complex value(s) added with noise of complex Gaussian Variable (N).

$$X = S + N \quad (2)$$

$$= \rho e^{j\theta} + N$$

$$X_R = S_R + N_R \quad (3)$$

$$X_I = \rho \cos(\theta) + N_I \quad (4)$$

$$X_I = S_I + N_I \quad (5)$$

$$X_I = \rho \sin(\theta) + N_I \quad (6)$$

Whereas ρ = Magnitude and θ is the phase. The probability Distribution Function of Real and Imaginary part of noise added signal is

$$f(X_R, X_I) = 1/\pi\sigma^2 e^{-(X_R - S_R)^2 + (X_I - S_I)^2 / 2\sigma^2} \quad (7)$$

σ is characterizing the magnitude of noise. To obtain PDF of the amplitude and Phase we go for polar coordinate systems

$$X_R = R \cos(\phi) \quad (8)$$

$$X_I = R \sin(\phi) \quad (9)$$

Equation for (7) with bivariate transform can be

shown as below

$$f(R, \phi) = R/2 \pi\sigma^2 e^{-(R^2 + \rho^2 - 2R\rho \cos(\phi - \theta)) / 2\sigma^2}$$

The marginal PDF of the intensity ($I=R^2$) is

$$f(I) = e^{-I + \rho^2 / 2\sigma^2} 2\sigma^2 * I_0(\rho\sqrt{I} / \sigma^2) \quad (10)$$

I is greater nor equal to 0

The marginal PDF of

Measured signal phase ($0 < \phi < 2\pi$)

$$\oint_0^{2\pi} f(R, \phi) dR \quad (11)$$

$$= 1/2\pi \oint_0^{2\pi} R \cdot \exp(-(R - \rho \cos(\phi - \theta))^2 / 2\sigma^2) + \rho^2 \sin^2(\phi - \theta) / dR \quad (12)$$

The above theoretical equations applied to the input signal and the plot of the signal shown in the figure 6(a), 6(b), and 6(c).

From the plots of PDF, the bin in the distribution chart shows more in number as the size of the cell increased. The size of the signal value area is proportional to the cell size.

The Standard normal distribution is a simplest normal distribution. In this distribution $\mu=0$ and $\sigma = 1$ and it is described by the PDF equation as below

$$\Phi(x) = \frac{1}{\sqrt{2\pi}} e^{-x^2/2} \quad (13)$$

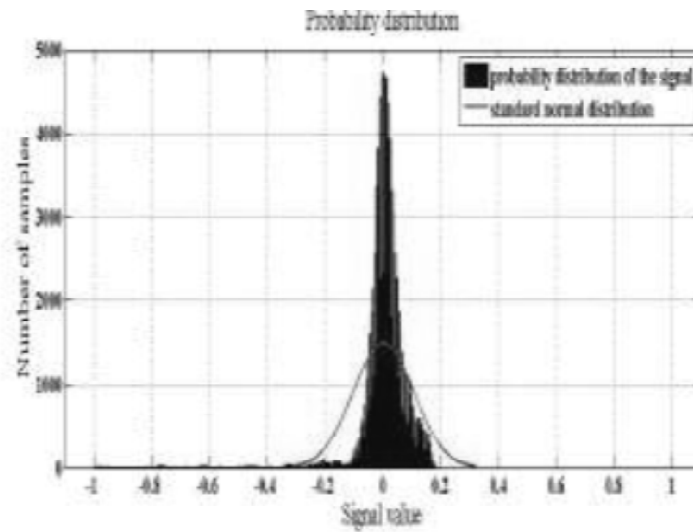


Figure 6(a): Probability distribution of the 1mm cancer cell signal

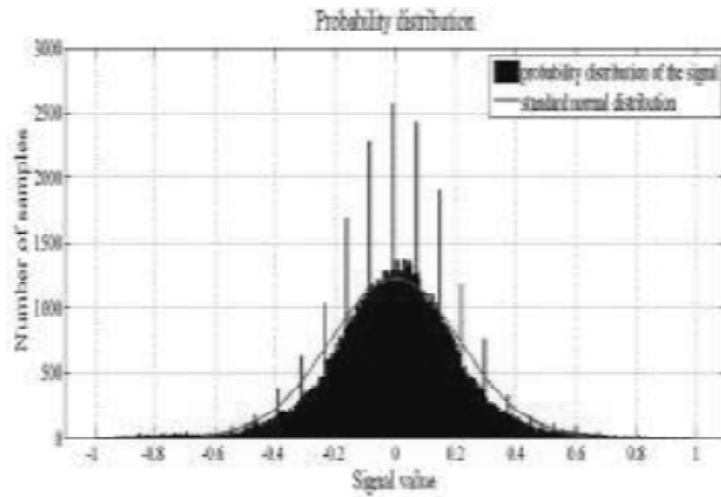


Figure 6(b): Probability distribution of the 2mm cancer cell signal

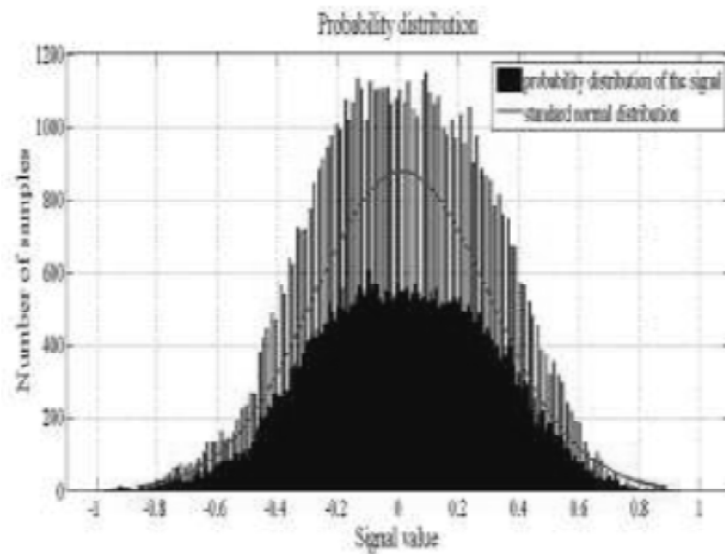


Figure 6(c): Probability distribution of the 5mm cancer cell signal

Whereas $1/\sqrt{2\pi}$ is equal to one under $\Phi(x)$ curvature. From the Figure 6(a),6(b) and 6(c) the standard normal distribution of curve is small and tall so the value of standard deviation is small, as the curve expands wider and shorter represent the greater standard value. The Table below shows the character features of the signal.

Table 1
Statistical values of back scattered signal as same location for different size of cells

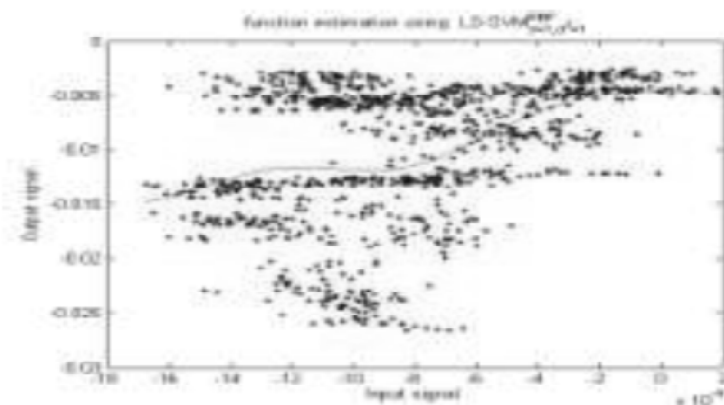
Cancer Cell	Sigma	Mu	Peak	Dynamic Range
1mm	0.10552	0.0024239	19.5313	53.0063
2mm	0.21383	0.0014768	13.3984	45.1536
3mm	0.21426	0.0018066	13.3809	36.5215
4mm	0.18822	0.0069649	14.5007	33.9794
5mm	0.29153	0.012622	10.6984	47.7121

From the Table 1, we can able to conclude that the standard deviation values are proportional to the size of the cells. The Table 2 shows the comparison of measured and experimentally calculated values.

Table 2
Comparison of measured and experimentally calculated values

Cancer Cell	Predicted
Measured Values	Cell Size Values(mm)
1mm	0.9840
2mm	1.9750
3mm	2.8682
4mm	3.9213
5mm	4.7832

The table shows how cancer cells size evaluated from backscattered signals to the actual size of the cells. The LSSVM regression methods applied to the collected data to avoid the shortcomings of classical methods. The Figure 7(a) shows the LSSVM regression for the datasets. The optimization obtains the weights in feature space, after the kernel function in the input samples, to measure the cancer cells



7(a) LSSVM of cancer cells of size 1mm

From the table, measurement of 2mm cancer cell results with increased values in variation compared to the other measure values.

CONCLUSION

The measurement and detection of cancer cell of size below 5mm, a challenging task. The problem approached with a novel technique, backscattering signals of NIR diodes. The nano size optical path length of signals correlated with the size of cells for detection and measurements. From the results, we conclude that the optical path length would performs well for detection of cell sizes below 5mm and an accuracy of 90% obtained from the datasets of 450 signals used for validations. Further, the work can be experimented with various frequencies of NIR diodes and can perfectly detected, for which frequency the size of cells would respond more compared NIR diodes with various wavelength.

REFERENCES

- [1] Paramkusham, S. ; Rao, K.M.M. ; Prabhakar Rao, B.V.V.S.N. "Early stage detection of breast cancer using novel image processing techniques, Matlab and Lab view implementation" 15th International Conference on Advanced Computing Technologies (ICACT), Sep-2013.
- [2] Karthikeyan Ganesan, U. Rajendra Acharya, Chua Kuang Chua, Lim Choo Min, K. Thomas Abraham, and Kwan-Hoong Ng "Computer-Aided Breast Cancer Detection Using Mammograms: A Review" *IEEE Reviews in Biomedical Engineering*, Vol. 6, 2013.
- [3] Asad, M, Azeemi, Naeem Zafar, Zafar, M.F, Naqvi, S.A. "Early Stage Breast Cancer Detection through Mammographic Feature Analysis" 5th International Conference on Bioinformatics and Biomedical Engineering, (iCBBE) -May2011.
- [4] Sura Ramzi Shareef "Breast Cancer Detection Based on Watershed Transformation" *IJCSI International Journal of Computer Science*, Issues, Vol. 11, Issue 1, No 1, January 2014.
- [5] S. Saheb Basha, Dr. K. Satya Prasa "Automatic detection of breast cancer mass in mammograms using morphological operators and fuzzy c –means clustering" *Journal of Theoretical and Applied Information Technology* © 2005 - 2009 JATIT. All rights reserved.
- [6] Lo, S.-C.B. ; Li, H. ; Yue Wang ; Kinnard, L "A multiple circular path convolution neural network system for detection of mammographic masses". *IEEE Transactions on Medical Imaging* (Impact Factor: 3.8). march 2002.
- [7] Lei Zhen ,A.K. Chan,"An artificial intelligent algorithm for tumor detection in screening mammogram" *IEEE Transactions on Medical Imaging*, Aug 2001.
- [8] Vishnukumar K. Patel, Syed Uvaid, A. C. Suthar,"Mammogram of Breast Cancer detection Based using Image Enhancement Algorithm" *International Journal of Emerging Technology and Advanced Engineering*, Volume 2, Issue 8, August 2012.
- [9] Wee Chang Khor , Bialkowski, M.E "Investigations into cylindrical and planar configurations of a microwave imaging system for breast cancer detection" *Antennas and Propagation Society International Symposium 2006*, IEEE.
- [10] A.M.Abbosh, M.E.Bialkowski,S.Crozier, "Investigations into optimum characteristics for the coupling medium in UWB breast cancer imaging systems" *Antennas and Propagation Society International Symposium*, 2008.IEEE
- [11] Heine JJ, Deans SR, Cullers DK, Stauduhar R, Clarke LP. "Multiresolution statistical analysis of high-resolution digital mammograms" *IEEE Trans Med Imaging*. OCT-1997.
- [12] Pouya Derakhshan-Barjoei, Mojdeh Bahadorzadeh, "Enhancement in Medical Image Processing for Breast Calcifications and Tumor Detection" *Research Journal of Applied Sciences, Engineering & Techonology*. Vol 4,issue 12, June 2012.
- [13] Ruey-Feng Chang, Chii-Jen chen; Ming-Feng Ho; Dar-Ren chen, "Breast ultrasound image classification using fractal analysis" *Fourth IEEE Symposium on Bioinformatics and Bioengineering*, 2004. BIBE 2004. Proceedings.